quaternary

MDPI

Article

Geological Records of a 1000-Yr-Old Extreme Tsunami Event Revealed by Drill Cores in Qiongzhou Strait

Chaoqun Wang [1], Xiaoxiao Yang [1,*], Lei Zhang [1], Yaoling Zhang [1], Dongxia Sun [1,2] and Daogong Hu [1]

[1] Institute of Geomechanics, Chinese Academy of Geological Sciences, Beijing 100081, China
[2] Key Laboratory of Active Tectonics and Geological Safety, Ministry of Natural Resources, Institute of Geomechanics, Chinese Academy of Geological Sciences, Beijing 100081, China
* Correspondence: yangxiaoxiao57@163.com

Abstract

In AD 1076, a super tsunami hit the South China Sea islands and the coasts of Guangdong and Vietnam. However, the impact on Hainan Island, situated farther from the tsunami source, remains unclear. Tsunami modeling indicates that seismic tsunamis from megathrust earthquakes in the Manila Subduction Zone may affect Guangdong, Hainan and Vietnam. This study found tsunami deposits in core HZK14 from southeastern Qiongzhou Strait, Hainan, characterized by increased grain-size anomalies, coexistence of young and old ages, and mixed microfossils from nearshore and middle-shelf settings. The youngest shell ^{14}C age from the core is AD 1100, which is close to the age of the AD 1076 tsunami event. Combined with geological records and historical documents, we conclude that tsunamis from the Manila Subduction Zone can reach Hainan's coast. This has significant implications for tsunami risk assessment and for the development of the Hainan Free Trade Zone. It also provides valuable constraints for tsunami simulations in the South China Sea.

Keywords: historical tsunami; geological record; ~1000 years ago; extreme tsunami event; Qiongzhou strait

1. Introduction

Tsunami hazards, triggered by submarine earthquakes, landslides, and volcanic eruptions, are considered among the deadliest marine disasters. Countries along the Pacific coast, including the United States, Canada, Chile, and Japan, have been repeatedly impacted by trans-Pacific tsunamis triggered by earthquakes and volcanic activities around the Pacific Rim [1–9]. The transoceanic tsunamis triggered by the 2004 Sumatra M_w 9.1 earthquake and the 2011 Japan M_w 9.0 earthquake caused significant damage to coastal residents and infrastructure, and also triggered environmental disasters [10–12]. These catastrophic marine events have attracted the attention of countries around the world to tsunami research.

Due to the physical conditions restricting tsunami generation, the eastern coast of China is minimally affected by tsunamis originating from the Pacific Ocean [13]. Meanwhile, the semi-enclosed tectonic environment of the South China Sea hinders the impact of external tsunami sources on its interior [14]. Tsunamis significantly impacting the Chinese coast primarily originate from earthquakes along the Manila subduction zone on the western side of the Philippines [15–18] and local tsunamis generated by earthquakes along the coastal fault zone in the northern South China Sea [19]. The occurrence of local tsunamis generated by earthquakes along the coastal fault zone is widely accepted [20,21]. Research on palaeotsunamis in the South China Sea indicates that tsunamis triggered by earthquakes

Check for updates

Academic Editor: Pedro Proença Cunha

Received: 19 July 2026
Revised: 25 August 2026
Accepted: 11 September 2026
Published: 16 September 2026

Copyright: © 2026 by the authors. Licensee MDPI, Basel, Switzerland. This article is an open access article distributed under the terms and conditions of the Creative Commons Attribution (CC BY) license.

in AD 1076 propagated to coastal countries in the South China Sea (Figure 1a). In addition to impacting the Philippines' Luzon Island, located near the tsunami source [22], the tsunami also struck the Xisha Islands and impacted the coasts of Guangdong and Hong Kong in China, causing the destruction of Nan'ao Song City [23–28], and the tsunami wave could reach Yongshu Reef in a southwest direction [29]. Tsunami simulations show that regardless of whether the Manila subduction zone ruptures as a whole or in segments, the resulting tsunamis would have catastrophic impacts on the coastal areas of Guangdong, Fujian, and Hainan, as well as the islands within the South China Sea [19]. However, there has been a lack of evidence for tsunami strikes along the northeastern coastline of Hainan Island in the past. Based on analyses of sedimentary structures, radiocarbon (^{14}C) and uranium-series (U-series) ages, geochemical proxies, and micropaleontological assemblages from core HZK14 in the southeastern Qiongzhou Strait (Figure 1b), this study confirms that the northeastern part of Hainan Island was struck by a tsunami approximately 1000 years ago. This finding provides crucial evidence for assessing the tsunami risk of Hainan Island and determining the extent of tsunami impact in the South China Sea.

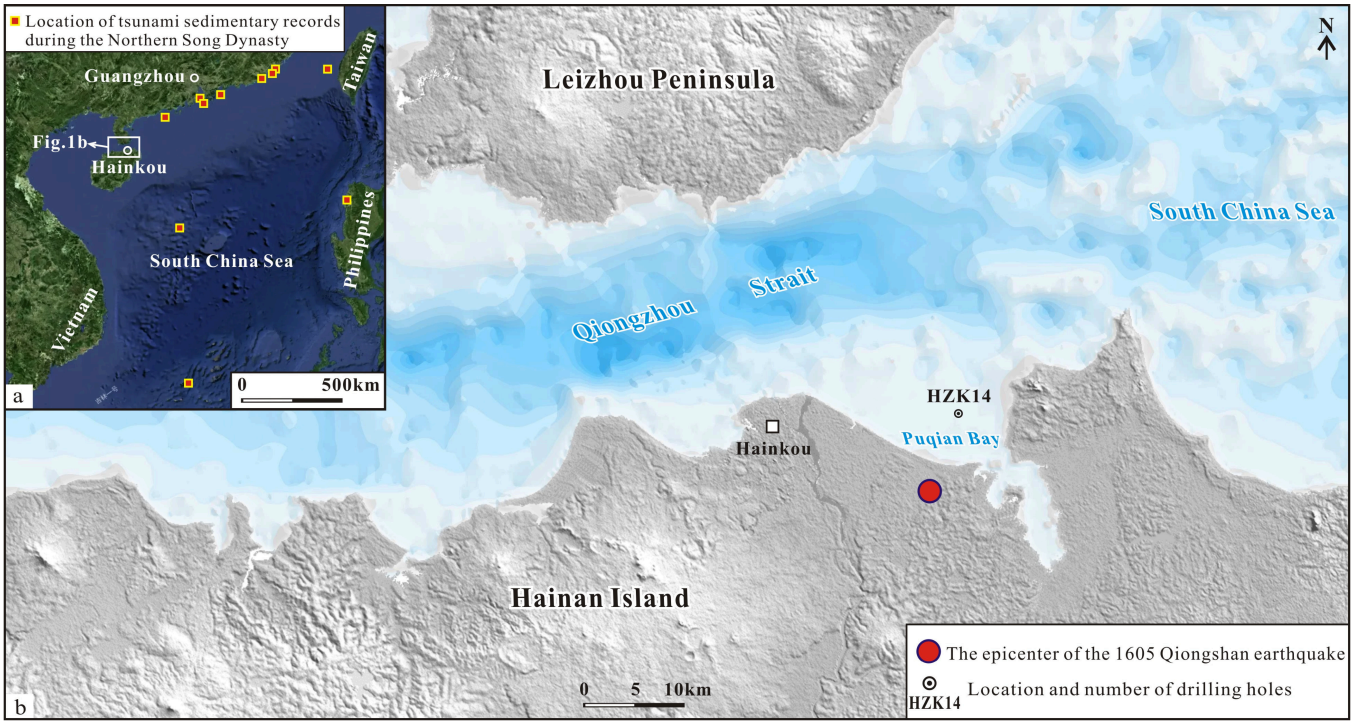


Figure 1. Location map of the study area and boreholes. (**a**) Location of tsunami records in AD 1076 [27]; (**b**) location of boreholes in Qiongzhou Strait.

2. Geological Background

The Qiongzhou Strait is located in the south of China, between Hainan Island and the Leizhou Peninsula. During the Late Quaternary, the Late Pleistocene Basuo Formation, characterized by fluvial facies, was deposited in the southeast of the Qiongzhou Strait. Due to the significant sea-level fall during the Last Glacial Maximum, the Late Pleistocene sediments were exposed and subjected to weathering and erosion, resulting in the formation of a mottled weathering crust. During the Holocene Megathermal, nearly 20-m-thick coastal swamp facies strata were deposited in the Qiongzhou Strait and Puqian Bay. Around 4400 years ago, sea level began to drop by approximately 2 m [30–32], causing Puqian Bay to transition into a river delta, through which the paleo-Sanjiang River (flowing across Dongzhai Port) discharged into the Qiongzhou Strait via the bay. The AD 1605 Qiongzhou earthquake induced vertical coseismic displacement along the Puqian-Qinglan Fault, fol-

lowed by long-term post-seismic creep, leading to a cumulative subsidence of up to 9 m in the southeast of Puqian Bay [21]. Consequently, geological records predating the AD 1605 earthquake have been well-preserved, minimally disturbed by subsequent human activities, making this area an ideal site for investigating historical tsunami events. Additionally, tsunami simulations indicate that this region is susceptible to tsunami wave inundation [19], suggesting a high potential for preserving tsunami deposits.

3. Methodology

3.1. Borehole Sediment Investigation

We drilled a core (HZK14) approximately 5.5 km from the coastline, at a site prior to paving, which was located on the southeastern margin of the Qiongzhou Strait at a water depth of about 8 m (Figure 2).

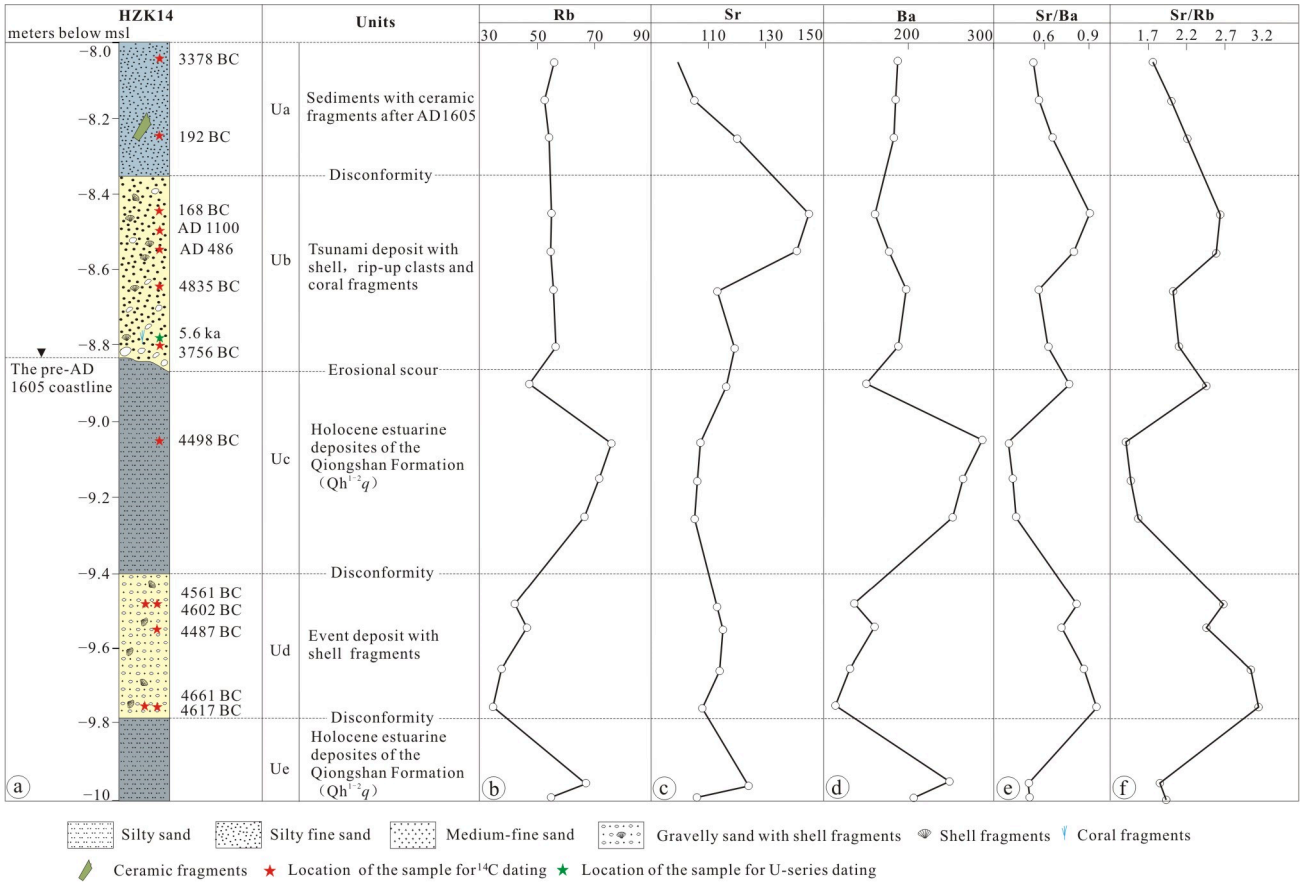


Figure 2. Stratigraphic columns and main geochemical indicators for the sediments of core HZK14. (**a**) Stratigraphic columns of rock cores from Borehole HZK14; (**b**) Trend of chemical element Rb variation along depth in Borehole HZK14; (**c**) Trend of Sr variation along depth in Borehole HZK14; (**d**) Trend of Ba variation along depth in Borehole HZK14; (**e**) Trend of Sr/Ba ratio variation along depth in Borehole HZK14; (**f**) Trend of Sr/Rb ratio variation along depth in Borehole HZK14.

The HZK14 core is composed of five sedimentary units arranged from top to bottom (Figure 2): Unit Ua (0~35 cm) comprises loose, uncemented gray silty sand, interspersed with ceramic fragments and shell fragments. Unit Ub (35~85 cm) consists of gray medium-fine sand containing shell, rip-up clasts, and coral fragments as well as subrounded quartzose gravels. Unit Ub is in erosional contact with the underlying Qiongshan Formation ($Qh^{1-2}q$). Unit Uc (85~140 cm) consists of dark gray silty sand of the Qiongshan Formation. Prior to the AD 1605 Qiongzhou earthquake, the strata were exposed at the surface, and Unit Ub was subsequently deposited unconformably atop Unit Uc. Unit Ud

(140~178 cm) is composed of yellowish-brown sand and gravel mixed with shell fragments, and is interpreted as an ancient tsunami or storm surge deposit. Unit Ue (178~200 cm) and Unit Uc have the same stratigraphic characteristics, and both are sedimentary strata of the Qiongshan Formation.

3.2. ^{14}C and U-Series Dating

Thirteen AMS ^{14}C dating samples were obtained from core HZK14 (Figure 2), spanning depths from 5 to 175 cm (Table 1). Of these, two samples originated from Unit Ua, five samples were derived from the coarse-grained event layer (Unit Ub), one from Unit Uc, and the remaining five from Unit Ud. Sample preparation was carried out by the Beijing Luminescence Laboratory Co., Ltd. The procedure involved the following steps: first, the outer and inner surfaces of each shell were mechanically abraded with a hand drill to remove adhered contaminants, followed by ultrasonic cleaning. The shells were then soaked in 1 M acetic acid for one day to eliminate any potential secondary carbonate contamination, after which they were rinsed with deionized water and oven-dried. An appropriate amount of each dried shell sample was weighed, and inorganic carbon was extracted using phosphoric acid and subsequently converted into elemental graphite using the CHS2-AGE3 system. The sample size was set to contain at least 1 mg of carbon to guarantee measurement reliability. After target preparation, the graphite targets were measured with a 200 kV MICADAS accelerator mass spectrometer (Ionplus AG, Dietikon, Switzerland) at the AMS ^{14}C Laboratory of Lanzhou University. Radiocarbon ages were calibrated using the Calib 8.2 software and the Marine 20 calibration curve, which is an independent international curve for the global marine reservoir [33,34]. Six ΔR values, three from the Xisha Islands and one each from Ho Chi Minh City, Con Dao Island, and Hon Tre Island in Vietnam [35–38] were selected from the MARINE20 database to calculate the ΔR (-155 ± 36 a) used for age correction.

Table 1. AMS ^{14}C ages of Shells in core HZK14.

Sample Number	Sample Depth (cm)	Units	Dating Material	Measured Age (a B.P.)	Corrected Age (95.4% Probability)	Median Corrected Age (BC/AD)
HZK14-4a	5	Ua	Bivalve shell	5001 ± 27	3556~3168 BC	3378 BC
HZK14-6	25		Bivalve shell	2467 ± 24	365 BC~AD 19	192 BC
HZK14-7	45	Ub	Bivalve shell	2449 ± 23	349 BC~AD 6	168 BC
HZK14-1	50		Bivalve shell	1315 ± 25	AD 951~1258	AD 1100
HZK14-8	55		Bivalve shell	1912 ± 23	AD 331~644	AD 486
HZK14-9	65		Bivalve shell	6356 ± 30	5026~4654 BC	4835 BC
HZK14-10	80		Bivalve shell	5364 ± 28	3938~3605 BC	3756 BC
HZK14-12	105	Uc	Bivalve shell	6057 ± 29	4675~4334 BC	4498 BC
HZK14-15a	148	Ud	Bivalve shell	6114 ± 29	4731~4373 BC	4561 BC
HZK14-15b	148		Bivalve shell	6152 ± 29	4784~4426 BC	4602 BC
HZK14-2	154		Bivalve shell	6047 ± 27	4665~4328 BC	4487 BC
HZK14-17a	175		Bivalve shell	6205 ± 29	4840~4474 BC	4661 BC
HZK14-17b	175		Bivalve shell	6166 ± 29	4795~4438 BC	4617 BC

One sample for U-series dating was taken from coral fragments at the bottom of Unit Ub of core HZK14 (Table 2). Samples analysis was conducted by the Key Laboratory of

Active Tectonics and Geological Safety, Ministry of Natural Resources. Age correction was applied using a coral-specific initial $^{230}Th/^{232}Th$ ratio of 0.5 ± 0.2.

Table 2. U-series ages of corals from Unit Ub of core HZK14.

Sample Number	U (ppm)	^{230}Th (mBq/g)	^{234}U (mBq/g)	^{232}Th (mBq/g)	$^{234}U/^{238}U$	$^{230}Th/^{232}Th$	$^{230}Th/^{234}U$	Measured Age (ka)	Corrected Age (ka)
HZK14-10	3.839	0.254 ± 0.016	3.450 ± 0.112	0.164 ± 0.012	1.211 ± 0.052	1.547 ± 0.143	0.074 ± 0.005	8.3 ± 3.7	5.6 ± 1.2

3.3. Geochemical Analysis

Based on the sediment grain size and fossil characteristics, eleven geochemical samples were collected from the core intervals of core HZK14 at depths of 5~125 cm (Table 3). All geochemical samples were analyzed at the National Research Center for Geoanalysis using a Rigaku-3080 X-ray Fluorescence Spectrometer (Rigaku Corporation, Akishima, Tokyo, Japan), with a precision of better than 0.5%. The trace elements Sr, Ba, Zn, and Rb were determined using a Rigaku-2100 spectrometer (Rigaku Corporation, Akishima, Tokyo, Japan), with analytical errors within 3–5%. The remaining trace elements were measured by a TJAPQ-ExCell ICP-MS (Beijing Haiguang Instrument Co., Ltd., Shunyi, Beijing, China), with analytical errors of less than 5% for elements with concentrations greater than 10×10^{-6}.

Table 3. Geochemical Element Concentrations and Ratios in Drill Cores from Qiongzhou Strait.

Sample Number	Depth/cm	Units	Element Concentration (μg/g)					Element Ratio	
			Ti	Mn	Sr	Ba	Rb	Sr/Ba	Sr/Rb
HZK14-4	5	Ua	1984	303	99.1	187	56.2	0.53	1.76
HZK14-5	15		1873	297	105	185	52.6	0.57	2.00
HZK14-6	25		1791	280	120	183	54.4	0.66	2.21
HZK14-7	45	Ub	1498	272	145	161	55	0.90	2.64
HZK14-8	55		1732	299	141	177	54.7	0.80	2.58
HZK14-9	65		2185	297	113	197	55.9	0.57	2.02
HZK14-10	80		2072	282	119	188	56.7	0.63	2.10
HZK14-11	90	Uc	1435	258	116	150	47.2	0.77	2.46
HZK14-12	105		3230	367	107	286	76.1	0.37	1.41
HZK14-13	115		3233	365	106	264	72	0.40	1.47
HZK14-14	125		2798	330	105	252	66.7	0.42	1.57

3.4. Microfossil Analysis

Based on unit divisions and grain-size variations, seven samples were collected from core HZK14 for micropaleontological analysis. Samples analysis was conducted by the Institute of Hydrogeology and Environmental Geology, Chinese Academy of Geological Sciences.

4. Test Results and Analysis

4.1. AMS ^{14}C and U-Series Dating Results

Tsunami waves, upon reaching the coast, often rapidly deposit heterogeneous marine sediments in coastal lowlands [39]. Tsunami deposits typically contain nearshore shell fragments, terrestrial animal remains, and deep-water marine microfossils [25,27,40,41]. To determine the deposition time of the tsunami layer, AMS ^{14}C dating was performed on marine or terrestrial organisms within the event layer, as well as in situ shells from the overlying and underlying strata. The AMS ^{14}C dating data and their calibration results for shells at 13 different depths from core HZK14 are presented in Table 1.

The AMS ^{14}C ages of two shells from sedimentary Unit Ua of core HZK14 are 192 BC and 3378 BC, respectively. The ^{14}C ages of five shells from sedimentary Unit Ub range from AD 1100 to 4835 BC, and exhibit age inversion and a phenomenon of mixed old and young ages within the same layer. The ^{14}C age of shells from the normal sedimentary deposits of the underlying Qiongshan Formation (Unit Uc) is 4498 BC. In contrast, five shell samples from the event layer (Unit Ud) yield ^{14}C ages of 4487 BC and 4661 BC, showing pronounced age inversions and a mixture of old and young materials, which probably represent a paleotsunami or storm surge event.

The U-series age of coral fragments from a depth of 80 cm at the base of Unit Ub in core HZK14 is 5.6 ± 1.2 ka (Table 2), which is close to the older ^{14}C age of shells from the same layer.

4.2. Geochemical Indicators

Offshore marine shells or substitutes for marine saltwater are more enriched in elements such as Ca, Sr, P, Ba, Mg, and Br, while sediments from terrestrial sources or deposited in high-energy hydrodynamic environments often accumulate TiO_2 and Zr, characterized by high contents of Al_2O_3 and Rb [27]. Therefore, element ratios and contents can serve as important indicators for identifying tsunami deposits [42].

Geochemical analysis of sediments from core HZK14 indicated that the Ti and Rb concentrations in Unit Ub are markedly lower than those in the underlying Unit Uc, but are comparable to those in the overlying sequence (Table 3, Figure 2). In contrast, Sr concentrations exhibit a positive anomaly in Unit Ub, whereas Ba concentrations remain similar to those in the overlying strata (Figure 2). Given that elemental concentrations are susceptible to grain-size variations, the Sr/Rb and Sr/Ba ratios can be used to correct for such grain-size effects, and thus the combined use of elemental ratios and absolute concentrations serves as a robust diagnostic proxy for paleo-tsunami events [43]. The average Sr/Ba ratio in four sediment samples from Unit Ub is 0.72 (Table 3), which is higher than the average Sr/Ba ratio of 0.56 in Chinese shallow sea sediments [27,44]. In contrast, the average Sr/Ba ratios in four samples from the underlying Unit Uc and three samples from the overlying Unit Ua are 0.49 and 0.58, respectively, lower than that in the Unit Ub deposit layer. The average Sr/Rb ratio in the Unit Ub is 2.35, also higher than the average Sr/Rb ratio of 1.72 in the Unit Uc sediments and the average Sr/Rb ratio of 1.99 in Unit Ua. These characteristics indicate that the Unit Ub layer was formed by the transport and accumulation of offshore sediments towards the shore, likely driven by tsunami waves. The average Ti content in the Unit Ub layer is 1871 μg/g, which is lower than the average Ti content of 2674 μg/g in the underlying Unit Uc sediments, as well as the average Ti content of 1882 μg/g in the overlying Unit Ua sediments.

4.3. Foraminiferal Records in the Deposits

In core HZK14, Unit Ua yields an abundance of 1232 specimens per 20 g of dry sediment. The dominant assemblage consists mainly of shallow-marine species, including *A. beccarii* (30.52%), *E. advenum* (12.34%), *P. armata* (7.79%), *Q. semimula* (5.84%), and *Q. akneriana* (5.84%).

The foraminiferal abundance in Unit Ub of core HZK14 reaches as high as 5344 specimens per 20 g, with 54 genera and 95 species identified. In Unit Ub, the predominant foraminifera fossil genera and species include *A. beccarii* (17.7%), *A. globosa* (2.1%), *E. advenum* (4.79%), *E. hispidulum* (1.8%), *P. armata* (11.98%), *Q. akneriana* (3.59%), *Q. semimula* (4.79%), *M. laevigata* (3.59%), and *T. inflata* (4.79%) (Figure 3), all indicative of shallow marine environments. Additionally, species typical of the middle continental shelf environment—including *C. magellanicum* (0.3%), *Q. costata* (5.09%), *Q. lamarckiana* (2.69%), *T. trigonula*

(5.69%), and *C. wuellerstorfi* (3.59%)—occur in relatively high proportions. Unit Uc has an abundance of 1070 specimens per 20 g, with the dominant assemblage again dominated by shallow-marine forms: *A. beccarii* (31.06%), *A. globosa* (6.48%), *A. tepida* (4.78%), *A. maruhasii* (9.56%), *E. advenum* (5.46%), *P. armata* (7.17%), and *T. inflata* (4.44%). Only minor occurrences of middle-continental-shelf indicators (*C. magellanicum* at 1.02%, *C. wuellerstorfi* at 0.68%, and *Q. lamarckiana* at 0.68%) are observed in this unit.

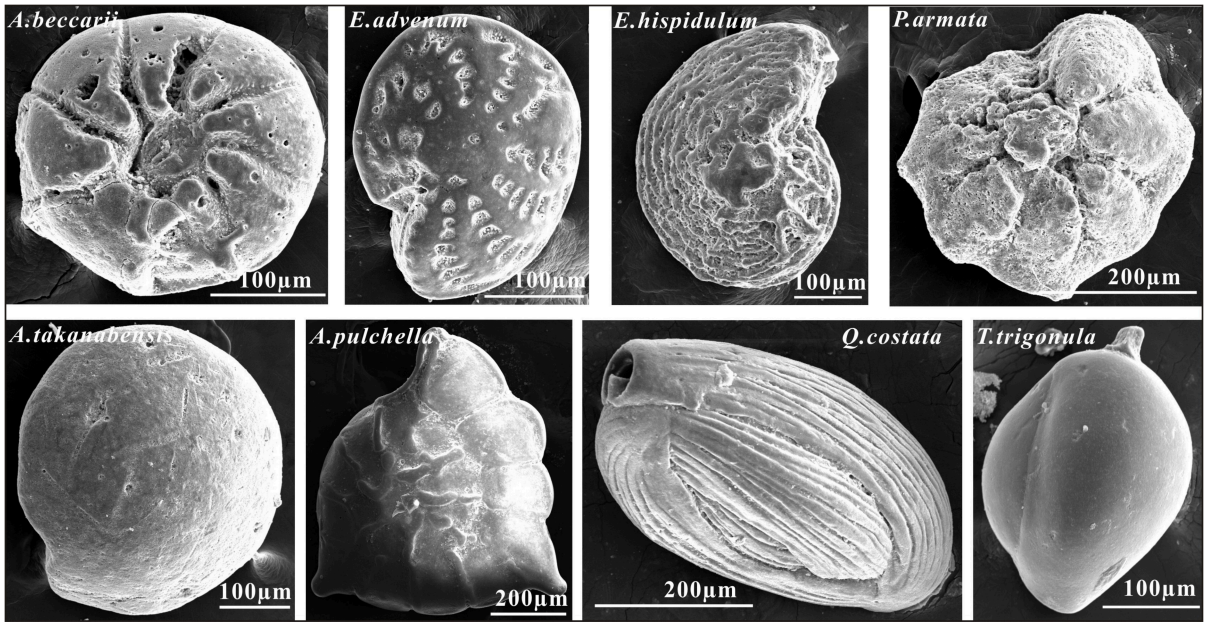


Figure 3. Foraminiferal fossils in the sediments of core HZK14.

Unit Ud shows an abundance of 2344 specimens per 20 g. The dominant assemblage is composed of shallow-marine taxa, chiefly *A. beccarii* (32.9%), *A. maruhasii* (6.73%), *E. advenum* (3.74%), *P. armata* (5.23%), and *T. inflata* (2.99%). Notably, this unit also contains elevated abundances of middle-continental-shelf species, including *A. takanabensis* (6.73%), *A. pulchella* (2.24%), *C. magellanicum* (2.24%), *P. tuberculatum* (3.74%), *Q. costata* (4.49%), and *T. trigonula* (2.99%).

5. Discussion

5.1. The Origin of Event Sediments in Marine Cores

The differentiation of tsunami deposits from storm deposits has been identified as one of the most challenging aspects of palaeotsunami event reconstruction [45]. Based on extensive research findings on tsunamis in modern, historical, and geological periods, scholars both domestically and internationally have summarized diagnostic evidence for tsunami deposits, including stratigraphy and sedimentology, provenance types, geochemical indicators, and microfossil evidence [26,41,45–50]. They believe that tsunami events can be effectively identified through the study of sedimentary structures, grain size variations, biological species, depositional ages, and geochemical indicators of the event layers.

Reconstructions of the sedimentary environment in Puqian Bay indicate that sea level began to fall at around 4400 cal yr BP [32], when it stood approximately 2 m higher than present, leading to a transition from marine to terrestrial conditions [31]. The great AD 1605 Qiongzhou earthquake then triggered substantial subsidence of 6 to 9 m in Puqian Bay [51,52], converting the area back to a marine setting and renewing sedimentation. Core observations from borehole HZK14 reveal that the event layer (Unit Ub) overlies the Holocene marine strata of the Qiongshan Formation, which were deposited prior to

4498 BC, indicating that these strata were subaerially exposed at the time of the event. The event layer was thus emplaced by storm-surge or tsunami overwash in an inland setting above the contemporary coastline, and was subsequently buried by sediments accumulated after the AD 1605 Qiongzhou earthquake.

Distinguishing between tsunami deposits and storm surge deposits is crucial for identifying ancient tsunamis [39]. In the northeastern part of Hainan Island, geological evidence for prehistoric extreme typhoons includes a shell ridge at Puqian Bay dating to approximately 4400 years ago and overwash deposits in coastal dunes dating to 3400 years ago [53,54]. Historical records also document several severe typhoon events: in AD 968, a typhoon struck Qiongzhou, "destroying city gates and nearly all government offices and houses," with similar events in AD 974 and AD 982 [55,56]. In AD 1501, a typhoon in Qiongshan caused storm surges with flooding and a water-level rise of about 2.2 m; in AD 1515, a strong northeast wind "swept seawater southwestward"; and in AD 1541, a gale "uprooted nearly all vegetation"; and in AD 1808, a severe typhoon generated storm surges that "extended from Puqian to Wushuling, more than ten li inland, killing over a dozen residents, and rendering the fields saline and uncultivable for years" (i.e., saltwater intrusion caused soil salinisation) [56]. These documentary accounts of typhoons are considered relatively reliable. Notably, the two major storm-surge events of AD 982 and AD 1808 are clearly recorded in cores HZK15 and HZK16 from Puqian Bay (data to be published elsewhere), whereas the smaller events have not yet been identified in the geological record.

In contrast, historical records of tsunamis are much scarcer, largely because tsunamis primarily affect coastal areas and ancient observers had limited understanding of such phenomena, potentially introducing biases in disaster documentation. Nevertheless, historical texts can still provide valuable clues for identifying past tsunamis. For example, the AD 1605 Qiongzhou earthquake caused seawater to inundate extensive areas that even the largest storm surges could not reach, and despite the event's tsunami-like characteristics, local chronicles and genealogies lack detailed descriptions [57]. In comparison, the AD 1076 event—which has been substantiated by event deposits along the South China Sea coast—was historically recorded as a major flood or a suspected tsunami [58].

Radiocarbon ages of reworked shells in event layers often predate or coincide with the actual timing of the tsunami [59]; the youngest shell age within an event layer can therefore be used as a proxy for the event age [60]. In our cores from the Qiongzhou Strait, the youngest age obtained from the event layer approximates the age of the AD 1076 tsunami, suggesting that this layer most likely represents the geological record of the AD 1076 earthquake-induced tsunami that reached Hainan Island.

In core HZK14, the Unit Ub is in erosional contact with the underlying Qiongshan Formation, which consists of grayish-green silty layers. In core HZK14, the Unit Ub is 50 cm thick and comprises gray medium-fine sand containing shell and coral fragments as well as subrounded quartzose gravels. Five shell radiocarbon ages range from AD 1100 to 3756 BC. These chronological data show coexistence of young and old values and exhibit age inversions, indicating a rapid depositional event.

The Unit Ub deposits preserved in core HZK14 are characterized by poor sorting, rip-up clasts from the underlying layers, a significant increase in particle size compared to the surrounding in situ layers, and coexistence of young and old ages, mixed microfossils from nearshore and middle-shelf settings, and geochemical anomalies. Notably, the middle-shelf microfossils recovered from core HZK14 are completely different from those found in the storm surge deposits of Puqian Bay, which are dominated by relatively shallow-water taxa such as *E. advenum*, *E. limpidum*, *A. beccarii*, and *A. maruhasii* [53]. In addition, the

presence of rip-up clasts from the underlying strata is a key criterion for identifying tsunami deposits [50]. All of these features are indicative of tsunami deposition [46–48,50].

5.2. Regional Evidence for the Timing of Tsunami Events

The median corrected ages of five shells from the tsunami layers in the core HZK14 in Qiongzhou Strait, obtained using AMS ^{14}C dating, range from 4835 BC to AD 1100. Tsunami deposits are event layers formed by rapid sedimentation upon wave arrival at the coast. Consequently, pre-existing "old" shells are often transported and redeposited by tsunamis, resulting in a mixture of old and young shell ages [27], the youngest shell age within the event layer is closer to the deposition age of the event. The youngest median corrected ^{14}C age of shells in the core HZK14 from Qiongzhou Strait is AD 1100. This age is close to the deposition ages of tsunami layers on Xisha East Island (AD 1017 to AD 1034), on Nan'ao Island (AD 1012 to AD 1072), and in the northern South China Sea (AD 1048 to AD 1108) [24,25,27].

5.3. Triggering Mechanisms of Tsunami Hazard Events

Studies have shown that most strong earthquakes in the coastal fault zone of the northern South China Sea are accompanied by tsunami phenomena. The Qiongzhou *M* 7½ earthquake that occurred near the Qiongzhou Strait in AD 1605 generated a local tsunami [57]. Sediments deposited after the earthquake-induced subsidence are present in Unit Ua (Figure 2), and further research is needed to determine whether these are tsunami deposits. Tsunamis that have had a significant impact on the Chinese coast originate from earthquakes in the Manila Subduction Zone [15,17]. Tsunami simulations indicate that earthquake-generated tsunamis originating from the Manila Subduction Zone are capable of striking the northeastern part of Hainan Island and the eastern entrance of the Qiongzhou Strait [19]. However, the impact of tsunamis triggered by the *M* 7½ earthquake in the Manila Subduction Zone on the southern coast of China is relatively low, with wave amplitudes generally not exceeding 30 cm [16,18]. Therefore, it can be inferred that the tsunami event in the southeast of Qiongzhou Strait, along with tsunami events recorded in the East Xisha Island, Nan'ao Island, and the northern waters of the South China Sea, was likely caused by a super tsunami triggered by a great earthquake of magnitude exceeding than *M* 7½ that occurred in the Manila Subduction Zone in AD 1076.

6. Conclusions

A tsunami deposit layer was identified in the core stratigraphy from the southeast of Qiongzhou Strait, Hainan Island. This layer is sharply differentiated from the underlying strata by its distinct sediment grain size, sedimentary structures, and facies. The deposit contains characteristic increased grain anomalies, shell fragments with mixed ages, mixed microfossils from nearshore and middle-shelf settings, indicating that the southeast of Qiongzhou Strait was situated on land above the contemporary coastline during the tsunami event. Both the land and tsunami layer exhibit subsidence of 8 to 10 m, attributed to the AD 1605 Qiongzhou earthquake. The youngest shell ^{14}C age from the core HZK14 is AD 1100, which is close to the age of the AD 1076 tsunami event in the South China Sea islands and coasts, as well as historical accounts of a major tsunami event in the South China Sea in AD 1076. These findings suggest that the northeastern part of Hainan Island and the Qiongzhou Strait were impacted by a tsunami in AD 1076. Consequently, the potential risk of damage to major coastal infrastructure projects from tsunamis triggered by large earthquakes in the Manila subduction zone deserves serious consideration.

Author Contributions: Conceptualization, C.W. and D.H.; methodology, C.W. and X.Y.; validation, Y.Z., D.S. and D.H.; formal analysis, C.W., X.Y. and L.Z.; investigation, C.W., X.Y. and L.Z.; resources,

C.W., X.Y. and L.Z.; data curation, C.W. and X.Y.; writing—original draft preparation, C.W. and X.Y.; writing—review and editing, C.W. and X.Y.; visualization, C.W. and X.Y.; supervision, D.H.; project administration, L.Z.; funding acquisition, L.Z. All authors have read and agreed to the published version of the manuscript.

Funding: This study is supported by Chinese Academy of Geological Sciences Basal Research Fund (No. JKYQN202412), the Institute of Geomechanics, Chinese Academy of Geological Sciences Basal Research Fund (No. DZLXJK202507) and Geological Survey project of China Geological Survey (No. DD202606201408).

Data Availability Statement: The raw data supporting the conclusions of this article will be made available by the authors on request.

Acknowledgments: We are grateful to the reviewers for their valuable comments.

Conflicts of Interest: The authors declare no conflicts of interest.

Abbreviations

The following abbreviations are used in this manuscript:

AMS	Accelerator Mass Spectrometry
ICP-MS	Inductively Coupled Plasma Mass Spectrometry
U-series ages	Uranium-series ages
AD	Anno Domini
BC	Before Christ

References

1. Atwater, B.F. Evidence for Great Holocene Earthquakes along the Outer Coast of Washington State. *Science* **1987**, *236*, 942–944. [CrossRef] [PubMed]
2. Atwater, B.F. Geologic evidence for earthquakes during the past 2000 years along the Copalis River Southern Coastal Washington. *J. Geophys. Res.* **1992**, *97*, 1901–1919. [CrossRef]
3. Darienzo, M.E.; Peterson, C.D. Episodic tectonic subsidence of late Holocene salt marshes, northern Oregon coast, central Cascadia margin, USA. *Tectonics* **1990**, *9*, 983–1014. [CrossRef]
4. Fujiwara, O.; Masuda, F.; Sakai, T.; Irizuki, T.; Fuse, K. Tsunami deposits in Holocene bay mud in southern Kanto region, Pacific coast of central Japan. *Sediment. Geol.* **2000**, *135*, 219–230. [CrossRef]
5. Nanayama, F.; Satake, K.; Furukawa, R.; Shimokawa, K.; Atwater, B.F.; Shigeno, K.; Yamaki, S. Unusually large earthquakes inferred from tsunami deposits along the Kuril trench. *Nature* **2003**, *424*, 660–663. [CrossRef] [PubMed]
6. Cisternas, M.; Atwater, B.F.; Torrejón, F.; Sawai, Y.; Machuca, G.; Lagos, M.; Eipert, A.; Youlton, C.; Salgado, I.; Kamataki, T.; et al. Predecessors of the giant 1960 Chile earthquake. *Nature* **2005**, *437*, 404–407. [CrossRef] [PubMed]
7. Monecke, K.; Finger, W.; Klarer, D.; Kongko, W.; McAdoo, B.G.; Moore, A.L.; Sudrajat, S.U. A 1000-year sediment record of tsunami recurrence in northern Sumatra. *Nature* **2008**, *455*, 1232–1234. [CrossRef]
8. Kitamura, A.; Kobayashi, K. Geologic evidence for prehistoric tsunamis and coseismic uplift during the ad 1854 Ansei-Tokai earthquake in Holocene sediments on the Shimizu Plain, central Japan. *Holocene* **2014**, *24*, 814–827. [CrossRef]
9. Rubin, C.M.; Horton, B.P.; Sieh, K.; Pilarczyk, J.E.; Daly, P.; Ismail, N.; Parnell, A.C. Highly variable recurrence of tsunamis in the 7400 years before the 2004 Indian Ocean tsunami. *Nat. Commun.* **2017**, *8*, 1619. [CrossRef] [PubMed]
10. Titov, V.; Rabinovich, A.B.; Mofjeld, H.O.; Thomson, R.E.; González, F.I. The global reach of the 26 December 2004 Sumatra tsunami. *Science* **2005**, *309*, 2045–2048. [CrossRef] [PubMed]
11. Goto, K.; Sugawara, D.; Abe, T.; Haraguchi, T.; Fujino, S. Liquefaction as an important source of the A.D.2011 Tohokuoki tsunami deposits at Sendai Plain, Japan. *Geology* **2012**, *40*, 887–890. [CrossRef]
12. Satake, K.; Heidarzadeh, M.; Quiroz, M.; Cienfuegos, R. History and features of trans-oceanic tsunamis and implications for paleo-tsunami studies. *Earth-Sci. Rev.* **2020**, *202*, 103112. [CrossRef]
13. Chen, Y.; Chen, Q.; Zhang, W. Tsunami disaster in China. *J. Nat. Disasters* **2007**, *16*, 1–6.
14. An, C. Tsunamis and tsunami warning: Recent progress and future prospects. *Sci. China Earth Sci.* **2021**, *64*, 191–204. [CrossRef]
15. Megawati, K.; Shaw, F.; Sieh, K.; Huang, Z.H.; Wu, T.R.; Lin, Y.N.; Tan, S.K.; Pan, T.C. Tsunami hazard from the subduction megathrust of the South China Sea: Part I. Source characterization and the resulting tsunami. *J. Asian Earth Sci.* **2009**, *36*, 13–20. [CrossRef]

16. Hong, M.L.; Huo, Z.X.; Ren, L.C. Study of the recurrence interval of *M7.5* earthquake in the middle part of Manila Trench in 1934 and modeling the Tsunami propagation induced by this earthquake. *J. Nanjing Norm. Univ. (Nat. Sci. Ed.)* **2016**, *39*, 8–13.
17. Hsu, Y.J.; Yu, S.B.; Loveless, J.P.; Bacolcol, T.; Solidum, R.; Jr, A.L.; Pelicano, A.; Woessner, J. Interseismic deformation and moment deficit along the Manila subduction zone and the Philippine Fault system. *J. Geophys Res.-Solid Earth* **2016**, *121*, 7639–7665. [CrossRef]
18. Liu, Y.N.; Wei, X.R.; Zhi, H.H.; Liu, J.W.; Li, P.L.; Bai, Y.F. Effects of potential seismic tsunamis in the Manila subduction zone onto coastal cities in South China. *Oceanol. Et Limnol. Sin.* **2023**, *65*, 331–350. [CrossRef]
19. Li, L.L.; Qiu, Q.; Li, Z.G.; Zhang, P.Z. Tsunami hazard assessment in the South China Sea:A review of recent progress and research gaps. *Sci. China Earth Sci.* **2022**, *52*, 803–831. [CrossRef]
20. Peng, C.G.; Li, Y.G.; Wu, M.B. Analysis of seismogenic structure mechanism of the Nanao earthquake in 1918. *South China J. Seismol.* **2017**, *37*, 1–14.
21. Xu, Q. The land sank into the sea and possible tsunami by the great earthquake in Qiongzhou in China in 1605. *Acta Oceanol. Sin.* **2007**, *29*, 146–156.
22. Ramos, N.T.; Maxwell, K.V.; Tsutsumi, H.; Chou, Y.C.; Duan, F.; Shen, C.C.; Satake, K. Occurrence of 1ka-old corals on an uplifted reef terrace in west Luzon, Philippines: Implications for a prehistoric extreme wave event in the South China Sea region. *Geosci. Lett.* **2017**, *4*, 12. [CrossRef]
23. Lu, C.H.; Yen, J.Y.; Chyi, S.J.; Yu, N.T.; Chen, J.H. Geological records of South China Sea tsunamis on Penghu Islands, Taiwan. *J. Asian Earth Sci.* **2019**, *177*, 263–274. [CrossRef]
24. Sun, L.G.; Zhou, X.; Huang, W.; Liu, X.; Yan, H.; Xie, Z.; Wu, Z.; Zhao, S.; Shao, D.; Yang, W. Preliminary evidence for a 1000-year-old tsunami in the South China Sea. *Sci. Rep.* **2013**, *3*, 1655. [CrossRef] [PubMed]
25. Yang, W.Q.; Sun, L.G.; Yang, Z.K.; Gao, S.; Gao, Y.S.; Shao, D.; Mei, Y.J.; Zang, J.J.; Wang, Y.H.; Xie, Z.Q. Nan'ao an archaeological site of Song dynasty destroyed by tsunami. *Chin. Sci. Bull.* **2019**, *64*, 107–120. [CrossRef]
26. Yang, W.Q.; Xie, Z.Q.; Sun, L.G. Research progress in the reconstruction of paleo-tsunami in theSouth China Sea and the tsunami deposit characteristics. *Earth Sci. Front.* **2021**, *28*, 246–257. [CrossRef]
27. Wang, Y.M.; Wang, Y.K.; Li, L.L.; Xu, Y.; Chen, X.H.; Zhang, P.Z. Paleo-tsunami sedimentary records and potential triggering mechanism during the Earlier Song Dynasty at the northern South China Sea. *Chin. Sci. Bull.* **2023**, *68*, 2690–2708. [CrossRef]
28. Xiong, H.; Zong, Y.; Huang, G.; Fu, S. Seabed erosion and deposition related to the typhoon activity of the past millennium on the southeast coast of China. *Earth Surf. Process Landf.* **2020**, *45*, 1695–1704. [CrossRef]
29. Yu, K.F.; Zhao, J.X.; Shi, Q.; Meng, Q.S. Reconstruction of storm/tsunami records over the last 4000 years using transported coral blocks and lagoon sediments in the southern South China Sea. *Quat. Int.* **2009**, *195*, 128–137. [CrossRef]
30. Wang, C.Q.; Jia, L.Y.; Hu, D.G.; Hu, J.M.; Zhang, L.; Yang, X.X.; Sun, D.X.; Mai, F.H.; Bai, S.B.; Zong, K.H.; et al. Quaternary activity characteristics of the Maniao-Puqian fault in the Jiangdong New District of Haikou. *Acta Geol. Sin.* **2022**, *96*, 403–417. [CrossRef]
31. Zhang, L.; Wang, C.Q.; Mai, F.H.; Jia, L.Y.; Sun, D.X.; Zhang, Y.L.; Yang, X.X.; Han, J.E.; Han, S.; Lü, T.Y.; et al. Maximum transgression paleocoastline in the Holocene in northern Hainan Island: Discovery and implications. *Geol. Rev.* **2023**, *68*, 2269–2276. [CrossRef]
32. Wang, Y.J.; Jiang, W.Y.; Yang, X.X.; Hu, D.G. Environmental changes over the last 39 ka as reconstructed from grain size characteristics of sediments in Dongzhaigang harbor, Hainan Island. *Quat. Sci.* **2024**, *44*, 1362–1370. [CrossRef]
33. Stuiver, M.; Reimer, P.J.; Braziunas, T.F. High-precision radiocarbon age calibration for terrestrial and marine samples. *Radiocarbon* **1998**, *40*, 1127–1151. [CrossRef]
34. Hajdas, I.; Ascough, P.; Garnett, M.H.; Fallon, S.J.; Pearson, C.L.; Quarta, G.; Spalding, K.L.; Yamaguchi, H.; Yoneda, M. Radiocarbon dating. *Nat. Rev. Methods Primers* **2021**, *1*, 62. [CrossRef]
35. Southon, J.; Kashgarian, M.; Fontugne, M.; Metivier, B.; Yim, W.S. Marine reservoir corrections for the Indian Ocean and Southeast Asia. *Radiocarbon* **2002**, *44*, 167–180. [CrossRef]
36. Dang, P.X.; Mitsuguchi, T.; Kitagawa, H.; Shibata, Y.; Kobayashi, T. Marine reservoir correction in the south of Vietnam estimated from an annually-banded coral. *Radiocarbon* **2004**, *46*, 657–660. [CrossRef]
37. Bolton, A.; Goodkin, N.F.; Druffel, E.R.M.; Griffin, S.; Murty, S.A. Upwelling of Pacific Intermediate Water in the South China Sea Revealed by Coral Radiocarbon Record. *Radiocarbon* **2016**, *58*, 37–53. [CrossRef]
38. Heaton, T.J.; Köhler, P.; Butzin, M.; Bard, E.; Reimer, R.W.; Austin, W.E.N.; Ramsey, C.B.; Grootes, P.M.; Hughen, K.A.; Kromer, B.; et al. Marine20-The marine radiocarbon age calibration curve (0-55000 cal BP). *Radiocarbon* **2020**, *62*, 779–820. [CrossRef]
39. Morton, R.A.; Gelfenbaum, G.; Jaffe, B.E. Physical criteria for distinguishing sandy tsunami and storm deposits using modern examples. *Sediment. Geol.* **2007**, *200*, 184–207. [CrossRef]
40. Dawson, A.G. Geomorphological effects of tsunami run-up and backwash. *Geomorphology* **1994**, *10*, 83–94. [CrossRef]
41. Dominey-Howes, D.T.M. Sedimentary deposits associated with the July 9th 1956 Aegean Sea tsunami. *Phys. Chem. Earth.* **1996**, *21*, 51–55. [CrossRef]

42. Chagué-Goff, C. Chemical signatures of palaeotsunamis:A forgotten proxy? *Mar. Geol.* **2010**, *271*, 67–71. [CrossRef]
43. Chagué-Goff, C.; Szczuciński, W.; Shinozaki, T. Applications of geochemistry in tsunami research: A review. *Earth-Sci. Rev.* **2017**, *165*, 203–244. [CrossRef]
44. Zhao, Y.Y.; Yan, M.C. Chemical element abundance in shallow sea sediments of China. *Sci. Chin. B Ser. B* **1993**, *23*, 1084–1090.
45. Zhang, Z.K.; Xie, L.; Yang, D.Y.; Yu, K.F. Progress in the study of tsunami deposits in the past 20 years. *Mar. Geol. Quat. Geol.* **2010**, *30*, 133–140. [CrossRef]
46. Dawson, A.G.; Stewart, I. Tsunami deposits in the geological record. *Sediment. Geol.* **2007**, *200*, 166–183. [CrossRef]
47. Nanayama, F.; Shigeno, K.; Satake, K.; Shimokawa, K.; Koitabashi, S.; Miyasaka, S.; Ishii, M. Sedimentary differences between the 1993 Hokkaido-nansei-oki tsunami and the 1959 Miyakojima typhoon at Taisei, southwestern Hokkaido, northern Japan. *Sediment. Geol.* **2000**, *135*, 255–264. [CrossRef]
48. Goff, J.; McFadgen, B.G.; Chagué-Goff, C. Sedimentary differences between the 2002 Easter storm and the 15th century Okoropunga tsunami, southeastern North Island, New Zealand. *Mar. Geol.* **2004**, *204*, 235–250. [CrossRef]
49. Qiu, Z.Y.; Han, X.Q.; Wang, Y.J.; Tao, C.H. Tsunami pre-warning and studies on the Quaternary paleo-tsunami records. *J. Mar. Sci.* **2009**, *27*, 67–72.
50. Sharrocks, P.D.; Peakall, J.; Hodgson, D.M.; Barlow, N.L.M. Tsunami versus storms: Diagnostic sedimentary criteria in coastal lakes, lagoons and sinkhole deposits. *Earth-Sci. Rev.* **2025**, *271*, 105277. [CrossRef]
51. Xu, Q.H. Formation and migration of Dongzhai port in the northern Hainan Island and the major Qiongzhou earthuake of 1605. *Seismol. Geol.* **1986**, *8*, 92–96.
52. Chen, E.M.; Huang, Y.Y. Characteristics of the seismic damage and analysis of the seismic structure of the 1605 great earthquake of Qiongzhou, Hainan Island. *Acta Seismol.* **1989**, *11*, 319–331.
53. Wang, C.Q.; Sun, D.X.; Zhang, Y.L.; Yang, X.X.; Zhang, L.; Hu, D.G. A 4400-Year-Old Extreme Paleo-Storm Surge Recorded in the Dongzhai Port Chenier, Hainan Island, China. *J. Geomech.* **2026**, *32*, 656–669. [CrossRef]
54. Xu, X.M.; Gao, S.; Zhou, L.; Yang, Y.; Wei, W.; Mei, Y.J.; Li, Y.N.; Wang, L.; Zhao, P.P.; Liu, Z.Q.; et al. Sedimentary records of extreme wave events on the northeastern Hainan Island coast, southern China. *Haiyang Xuebao* **2019**, *41*, 48–63.
55. Ruan, Y. *Guangdong Tongzhi: Previous Events Summary*; Guangdong People's Publishing House: Guangzhou, China, 1981. (In Chinese)
56. Hong, S.X. *Daoguang Guangdong Tongzhi: Qiongzhou Prefecture*; Hainan Publishing House: Haikou, China, 2006. (In Chinese)
57. Xu, Q. The coseismic coast fast sinkage and the following possible tsunami caused by the 1605 Qiongshan strong earthquake and the evidence. *South China J. Seismol.* **2006**, *26*, 17–28.
58. Mak, S.; Chan, L.S. Historical tsunamis in South China. *Nat. Hazards* **2007**, *43*, 147–164. [CrossRef]
59. Bondevik, S.; Svendsen, J.I.; Johnsen, G.; Mangerud, J.; Kaland, P.E. The Storegga Tsunami Along the Norwegian Coast, Its Age and Run Up. *Boreas* **1997**, *26*, 29–53. [CrossRef]
60. Ishizawa, T.; Goto, K.; Yokoyama, Y.; Goff, J. Dating tsunami deposits: Present knowledge and challenges. *Earth-Sci. Rev.* **2020**, *200*, 102971. [CrossRef]

Disclaimer/Publisher's Note: The statements, opinions and data contained in all publications are solely those of the individual author(s) and contributor(s) and not of MDPI and/or the editor(s). MDPI and/or the editor(s) disclaim responsibility for any injury to people or property resulting from any ideas, methods, instructions or products referred to in the content.